Physics Letters B 758 (2016) 389–401

Contents lists available at ScienceDirect

Physics Letters B

www.elsevier.com/locate/physletb

Multi-strange baryon production in p–Pb collisions at $\sqrt{s_{\rm NN}} = 5.02$ TeV

ALICE Collaboration *

ARTICLE INFO

Article history:
Received 16 January 2016
Received in revised form 10 May 2016
Accepted 10 May 2016
Available online 12 May 2016
Editor: L. Rolandi

ABSTRACT

The multi-strange baryon yields in Pb–Pb collisions have been shown to exhibit an enhancement relative to pp reactions. In this work, Ξ and Ω production rates have been measured with the ALICE experiment as a function of transverse momentum, $p_{\rm T}$, in p–Pb collisions at a centre-of-mass energy of $\sqrt{s_{\rm NN}} = 5.02$ TeV. The results cover the kinematic ranges 0.6 GeV/c < $p_{\rm T}$ < 7.2 GeV/c and 0.8 GeV/c < $p_{\rm T}$ < 5 GeV/c, for Ξ and Ω respectively, in the common rapidity interval $-0.5 < y_{\rm CMS} < 0$. Multi-strange baryons have been identified by reconstructing their weak decays into charged particles. The $p_{\rm T}$ spectra are analysed as a function of event charged-particle multiplicity, which in p–Pb collisions ranges over one order of magnitude and lies between those observed in pp and Pb–Pb collisions. The measured $p_{\rm T}$ distributions are compared to the expectations from a Blast-Wave model. The parameters which describe the production of lighter hadron species also describe the hyperon spectra in high multiplicity p–Pb collisions. The yield of hyperons relative to charged pions is studied and compared with results from pp and Pb–Pb collisions. A continuous increase in the yield ratios as a function of multiplicity is observed in p–Pb data, the values of which range from those measured in minimum bias pp to the ones in Pb–Pb collisions. A statistical model qualitatively describes this multiplicity dependence using a canonical suppression mechanism, in which the small volume causes a relative reduction of hadron production dependent on the strangeness content of the hyperon.

© 2016 The Author(s). Published by Elsevier B.V. This is an open access article under the CC BY license (http://creativecommons.org/licenses/by/4.0/). Funded by SCOAP[3].

1. Introduction

Collisions of heavy nuclei at ultra-relativistic energies allow the study of a deconfined state of matter, the Quark–Gluon Plasma, in which the degrees of freedom are partonic, rather than hadronic. The role of strange hadron yields in searching for this state was pointed out at an early stage [1]. It was subsequently found that in high energy nucleus–nucleus (A–A) collisions at the Super Proton Synchrotron (SPS), the Relativistic Heavy Ion Collider (RHIC) and the Large Hadron Collider (LHC) the abundances of strange and multi-strange baryons are compatible with those from thermal statistical model calculations [2–10].

In smaller collision systems at the same centre-of-mass energies, in particular proton–proton (pp) collisions, the relative abundance of multi-strange baryons is lower with respect to A–A collisions, whether normalised to participant nucleons or produced particles (pions or charged hadrons). This led to the interpretation that strangeness enhancement is observed in A–A collisions. Attempts to explain this phenomenon include the application of a canonical formalism in the statistical model, replacing the grand canonical approach, in which the requirement to conserve the strangeness quantum number when producing (multi-)strange baryons in small systems is imposed [11]. This means that strange hadrons are produced with a lower relative abundance in small systems, an effect known as canonical suppression. Such a theoretical framework has been used to make predictions for LHC energies [12]. Further complications in the interpretation arise when the produced system, although small, is formed in peripheral A–A collisions where the particle production may not be from a contiguous volume due to core-corona effects [13,14]. Evidence for this effect was seen at RHIC where a canonical suppression calculation based on the estimated number of participant nucleons could not successfully reproduce the data [15]. A cleaner way to investigate canonical suppression effects is provided by proton–nucleus (p–A) collisions.

Proton–nucleus collisions provide an opportunity to study the $p_{\rm T}$-dependence of the particle spectra created in a system with a different, more compact, initial geometry than A–A collisions where a similar number of charged particles are produced. Studying this dependence is important in determining the applicability of hydrodynamics [16] which has been successful in describing the particle spectra in A–A collisions [17–19].

At the LHC the combination of the rise in particle production per nucleon–nucleon collision with increasing $\sqrt{s}$ and a dedicated p–Pb data-taking period have enabled the ALICE experiment to

* *E-mail address:* alice-publications@cern.ch.

http://dx.doi.org/10.1016/j.physletb.2016.05.027
0370-2693/© 2016 The Author(s). Published by Elsevier B.V. This is an open access article under the CC BY license (http://creativecommons.org/licenses/by/4.0/). Funded by SCOAP[3].

collect a large sample of $\Xi^{\pm}$ and $\Omega^{\pm}$. In this Letter, we set out the methods for these studies, present the results obtained and discuss how they fit into a theoretical picture.

2. Sample and data analysis

The results presented in this Letter were obtained from a sample of the data collected with the ALICE detector [20] during the LHC p–Pb run at $\sqrt{s_{\rm NN}} = 5.02$ TeV in the beginning of 2013. The two scintillator arrays V0A (direction of Pb beam), and V0C (direction of p beam), covering pseudo-rapidity ranges of $2.8 < \eta < 5.1$ and $-3.7 < \eta < -1.7$, respectively, served both as triggering detectors and for determining the event multiplicity class [21]. The tracking of particles in the central barrel, covering $|\eta| < 0.9$, takes place in the Inner Tracking System (ITS), which consists of the two innermost silicon pixel layers, surrounded by two silicon drift and two silicon strip layers, all placed within a radius of 43 cm, and the Time Projection Chamber (TPC), a large cylindrical drift chamber filled with a Ne–CO_2 gas mixture [20]. Measurements of the energy loss by charged particles in the gas allow particles to be identified with this detector.

A trigger requiring a coincidence within less than 1 ns in the V0 detectors selected around 100 million events, which are mainly non-single diffractive (NSD) events and contain a negligible contribution from single diffractive (SD) and electromagnetic (EM) processes [22]. A dedicated radiator-quartz detector (T0) provided a measurement of the event time of the collisions. The V0 and T0 time resolutions allowed discrimination of beam–beam interactions from background events in the interaction region. Further background suppression was applied in the offline analysis using time information from the neutron Zero Degree Calorimeter on the Pb-going side. Primary vertices (PVs) were selected if their position along the beam axis was reconstructed within 10 cm of the geometrical centre of the detector. In Monte Carlo (MC) studies an efficiency of 99.2% for this trigger was obtained, while the joint trigger and primary vertex reconstruction efficiency lies at 97.8% [22]. The estimated mean number of interactions per bunch crossing was below 1% in the sample chosen for this analysis.

The analysed events were divided into seven multiplicity percentile classes according to the total number of particles measured in the forward V0A detector. The efficiency-corrected mean number of charged primary particles per unit rapidity ($\langle {\rm d}N_{\rm ch}/{\rm d}\eta \rangle$) within $-0.5 < \eta < 0.5$ in the laboratory reference frame for each of these multiplicity bins were published in [23].

Due to the asymmetric energies of the proton and lead ion beams, a consequence of the 2-in-1 magnet design of the LHC, the nucleon–nucleon centre-of-mass system is shifted by 0.465 units of rapidity in the direction of the proton beam with respect to the laboratory frame. The measurements reported in this Letter were performed in the central rapidity window defined in the centre-of-mass frame within $-0.5 < y < 0$, where negative rapidity corresponds to the side of the detector into which the Pb beam travels.

The identification of multi-strange baryons was based on the topology of their weak decays through the reconstruction of the tracks left behind by the decay products, referred to as the daughter particles. The daughters of the $\Xi^- \to \Lambda\pi^-$ (BR: 99.9%), $\Omega^- \to \Lambda K^-$ (BR: 67.8%) and the subsequent $\Lambda \to p\pi^-$ (BR: 63.9%) weak decays [24], as well as the corresponding decays of the $\overline{\Xi}^+$ and $\overline{\Omega}^+$, were reconstructed by combining track information from the TPC and the ITS [25]. Proton, anti-proton and charged π and K tracks were identified in the TPC via their measured energy deposition, which was compared with a mass-dependent parameterisation of ionisation loss in the TPC gas as a function of momentum [26]. All daughter candidates were required to lie within 4σ of their characteristic Bethe–Bloch energy loss curve. Multi-strange candidates were selected through the geometrical association of the V^0 component (Λ or $\bar{\Lambda}$ decay) to a further secondary, 'bachelor' track (identified as $\pi^{\pm}$ or $\rm K^{\pm}$). In this process, several geometrical variables were measured for each candidate, and criteria were set on them in order to purify the selected sample: numerical values for the selection cuts applied are reported in Table 1. These selections are similar to those in the pp measurements [25], a consequence of the low multiplicities present in the detector in the p–Pb collisions. As a result the correction factors for the efficiency are also similar. In addition to the settings on topological variables, a cut has been applied on the V^0 invariant mass window of ± 8 MeV/c^2 from the nominal Λ mass [24]. Further restrictions were set on the proper lifetime of the $\Xi^{\pm}$ and $\Omega^{\pm}$. By requiring this variable to be less than 3 times the mean decay length (4.91 cm and 2.46 cm, respectively), we discarded low-momentum secondary particles and false multi-strange candidates, the daughter tracks of which originated from interactions with detector material.

Table 1
The parameters for V^0 (Λ and $\bar{\Lambda}$) and cascades ($\Xi^{\pm}$ and $\Omega^{\pm}$) selection criteria. Where a criterion for $\Xi^{\pm}$ and $\Omega^{\pm}$ finding differs, the value for the $\Omega^{\pm}$ case is in parentheses. DCA represents "distance of closest approach," PV the primary vertex, θ is the angle between the momentum vector of the reconstructed V^0 or cascade, and the displacement vector between the decay and primary vertices. The curvature of the cascade particle's trajectory is neglected.

V^0 finding criteria	
DCA: $h^{\pm}$ to PV	> 0.04 (0.03) cm
DCA: h^- to h^+	< 1.5 standard deviations
Λ mass ($m_{\rm V0}$)	$1.108 < m_{\rm V0} < 1.124$ GeV/c^2
Fiducial volume ($R_{\rm 2D}$)	$R_{\rm 2D} > 1.1$ (1.2) cm
V^0 pointing angle	$\cos\theta_{\rm V0} > 0.97$
Cascade finding criteria	
Proper decay length	$< 3\times$ mean decay length
DCA: $\pi^{\pm}$ ($K^{\pm}$) to PV	> 0.04 cm
DCA: V^0 to PV	> 0.06 cm
DCA: $\pi^{\pm}$ ($K^{\pm}$) to V^0	< 1.3 cm
Fiducial volume ($R_{\rm 2D}$)	$R_{\rm 2D} > 0.5(0.6)$ cm
Cascade pointing angle	$\cos\theta_{\rm casc} > 0.97$

The invariant mass of the Ξ and Ω hyperons was calculated by assuming the known masses [24] of the Λ and of the bachelor track. The mass was reconstructed twice for each cascade candidate, once assuming the bachelor to be a π and once a K. This allowed the removal of an important fraction of the Ω background, which contained a large contribution from the Ξ candidates that pass the Ω selection criteria. Most of these false Ω were removed discarding all candidates that could be reconstructed as Ξ with a mass within 10 MeV/c^2 of the known mass [24] of the Ξ baryon. Fig. 1 shows the invariant mass distributions for the Ξ^- and Ω^- hadrons in well populated $p_{\rm T}$ bins for the lowest and highest multiplicity classes.

For the signal extraction, a peak region was defined within 4σ of the mean of a Gaussian invariant mass peak for every measured $p_{\rm T}$ interval. Adjacent background bands, covering an equal combined mass interval as the peak region, were defined on both sides of that central region. This is illustrated in Fig. 1 with the shaded bands on either side of the peak. The number of bin entries inside the side-bands was subtracted from the number of candidates within the peak region, assuming the background to be linear across the mass range considered.

The $p_{\rm T}$ distributions were corrected for detector acceptance and reconstruction efficiencies. These were estimated with the use of DPMJet [27] simulated Monte Carlo (MC) events, which were propagated through the detector with GEANT3 [28].

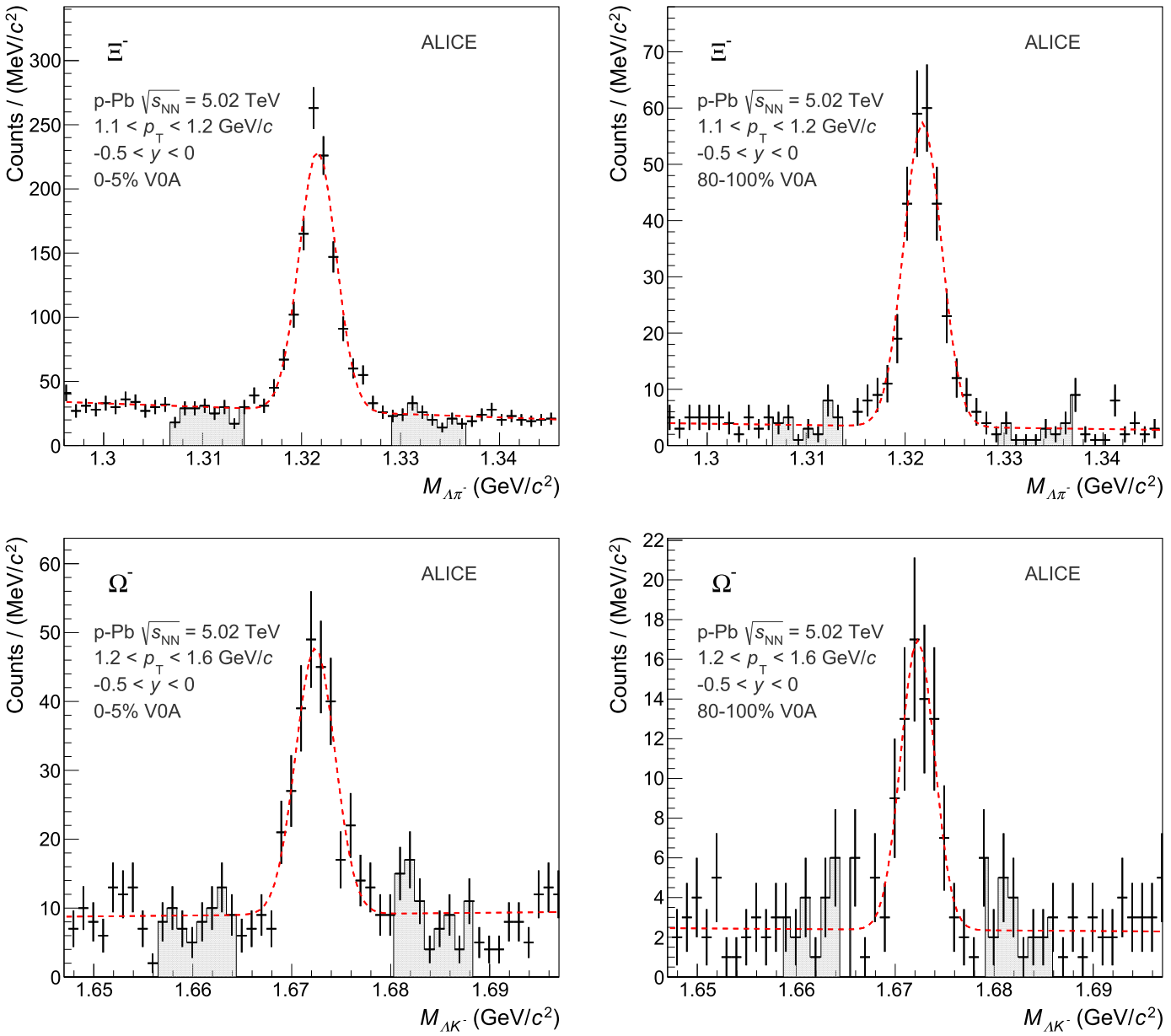

Fig. 1. Invariant mass distributions of the Ξ^- and Ω^- in the 1.1–1.2 GeV/c and 1.2–1.6 GeV/c p_{T} bins respectively, fitted with a Gaussian peak and linear background (dashed red curves). The distributions for highest (left) and lowest (right) multiplicity classes are shown. The fits only serve to illustrate the peak position with respect to which the bands were defined and the linear background assumption for the applied signal extraction method.

2.1. Systematic uncertainties

Systematic uncertainties due to the choice of selection criteria were examined separately in each p_{T} interval of the measured spectra. Individual settings were loosened and tightened, in order to measure changes in the signal loss correction. For the Ξ hyperons, the signal extraction accounts for an uncertainty of around 2% but reaches 5% at low-p_{T} and in high multiplicity events, while for the Ω, uncertainties of 3–5% were measured. The uncertainty due to the topological selections is around 2(3)% for the main p_{T} region, and up to 3(5)% at low momentum for $\Xi(\Omega)$. The constraint on the V^0 mass window contributes to the total uncertainty with around 0.5(1)% and both the TPC tracking and identification cuts with 2(3)%. The proper decay length cut gives another 3(5)% uncertainty at low p_{T}. A 4% error was added due to the material budget, and for the $\Omega^{\pm}$ only, an additional 3% due to the mass hypothesis cut. All these individual error contributions, which are listed in Table 2, are added in quadrature. Apart from the low momentum region, no p_{T} dependence is observed in the total uncertainty. The total systematic error lies between 5–6(8)% across the whole spectrum, reaching up to 8(14)% in the lowest p_{T} bins for the $\Xi(\Omega)$ baryons.

The fraction of the systematic error that is uncorrelated across multiplicity was calculated by using the same method applied in [23], in which spectra deviations in specific multiplicity classes were compared to those observed in the integrated data sample. The choice of the topological parameter values and the applied signal extraction method generates the dominant contribution to the uncorrelated uncertainties across multiplicity. These uncertainties were measured to be within 2% in the case of the Ξ and 3% in the case of the Ω, which constitutes a fraction that lies between 20 and 40% of the total systematic uncertainties.

Table 2
Contributions to the total systematic uncertainties for the $\Xi^{\pm}$ and $\Omega^{\pm}$ spectra measurements. The values in brackets indicate the maximum uncertainties measured for low-p_{T} cascades (see text).

Source	$\Xi^{\pm}$	$\Omega^{\pm}$
Material budget	4%	4%
Competing mass hypothesis	–	3%
Topological variables	2–3(5)%	3–5%
Signal extraction	2(5)%	3(5)%
Particle identification	2%	3%
Track selection	2%	3%
Proper decay length	1(3)%	2(5)%
V^0 mass window	0.5%	1%

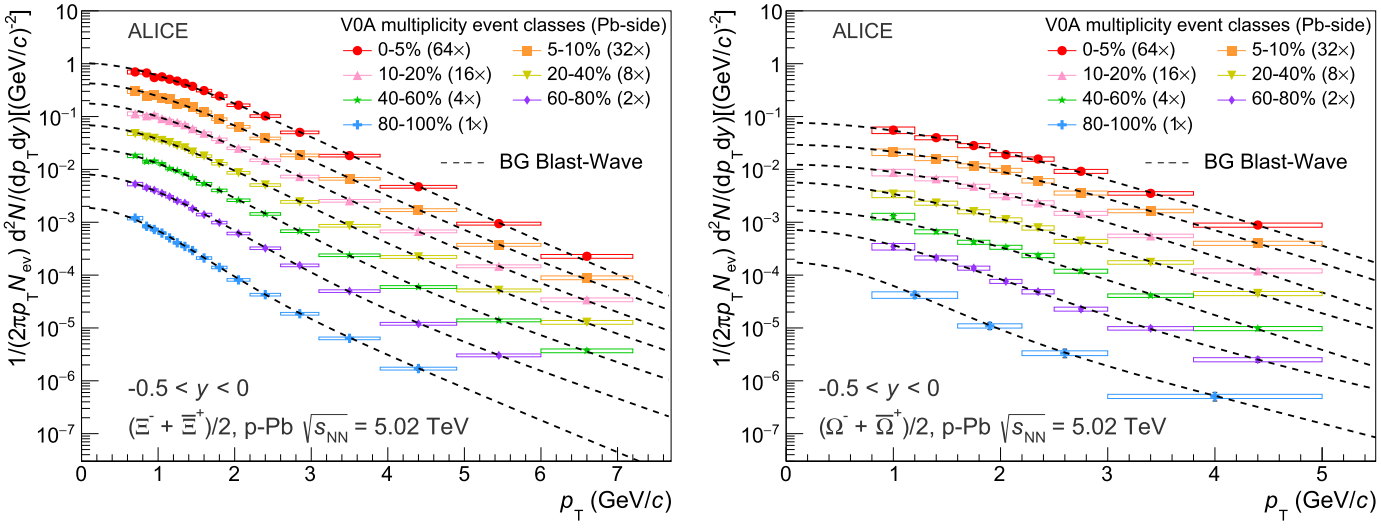

Fig. 2. (Colour online.) Invariant p_{T}-differential yields of $(\Xi^- + \overline{\Xi}^+)/2$ and $(\Omega^- + \overline{\Omega}^+)/2$ in different multiplicity classes. Data have been scaled by successive factors of 2 for better visibility. Statistical (bars), full systematic (boxes) and uncorrelated across multiplicity (transparent boxes) uncertainties are plotted. The dashed curves represent Blast-Wave fits to each individual distribution.

3. Results

3.1. Transverse momentum spectra

The p_{T} distributions of Ξ^-, $\overline{\Xi}^+$, Ω^- and $\overline{\Omega}^+$ in $-0.5 < y < 0$ are shown in Fig. 2 for different multiplicity intervals, as defined in [23]. Since antiparticle and particle spectra are identical within uncertainties, the average of the two is shown. The spectra exhibit a progressive flattening with increasing multiplicity, which is qualitatively reminiscent of what is observed in Pb–Pb collisions [10].

The calculation of p_{T}-integrated yields can be performed by using data in the measured region and a parametrisation-based extrapolation elsewhere. The Boltzmann–Gibbs Blast-Wave (BG–BW) model [16] gives a good description of each p_{T} spectrum and has been used as a tool for this extrapolation. Other alternatives, such as the Levy–Tsallis [29] and Boltzmann distributions, were used for estimating the systematic uncertainty due to the extrapolation.

The extrapolation in the unmeasured $\Xi^{\pm}$ ($\Omega^{\pm}$) low-p_{T} region grows progressively with decreasing multiplicity, from around 16%(19%) of the total yield in the 0–5% multiplicity class to around 27%(40%) in the 80–100% class. The systematic uncertainty assigned to the yield due to the extrapolation technique is 2.8%(7.8%) for high multiplicities and rises to 5.2%(14.5%) in the case where the fraction of the extrapolated yield is highest.

3.2. Comparison to Blast-Wave model

In order to investigate whether the observed spectral shapes are consistent with a system that exhibits hydrodynamical radial expansion, the measured distributions have been further studied in the context of the BG–BW model [16]. This model assumes a locally thermalised medium that expands collectively with a common velocity field and then undergoes an instantaneous freeze-out. In this framework, a simultaneous fit to identified particle spectra allows for the determination of common freeze-out parameters. These can be used to predict the p_{T} distribution for other particle species in a collective expansion picture. It should be noted that such a simultaneous fit differs from the individual fits mentioned in the previous section and used only for extrapolating the spectra.

The Ξ^-, $\overline{\Xi}^+$, Ω^- and $\overline{\Omega}^+$ p_{T} spectra in the 0–5% and 80–100% multiplicity classes are compared to predictions from the BG–BW model with parameters acquired from a simultaneous fit to $\pi^{\pm}$, $\mathrm{K}^{\pm}$, $\mathrm{p}(\overline{\mathrm{p}})$ and $\Lambda(\bar{\Lambda})$ in Fig. 3 [23]. The model describes the measured shapes within uncertainties up to a p_{T} of approximately 4 GeV/c for Ξ and 5 GeV/c for Ω in the highest multiplicity class. This indicates that multi-strange hadrons also follow a common motion with the lighter hadrons and is suggestive of the presence of radial flow in p–Pb collisions. However, it is worth noting that some final state effects could also modify the spectra in a similar manner to radial flow. For example, PYTHIA [30] implements the colour reconnection mechanism, which fuses strings originating from independent parton interactions, leading to fewer but more energetic hadrons, which has been shown to mimic radial flow [31].

Applying the same technique to results from the lower multiplicity classes reveals that the agreement of the data with the

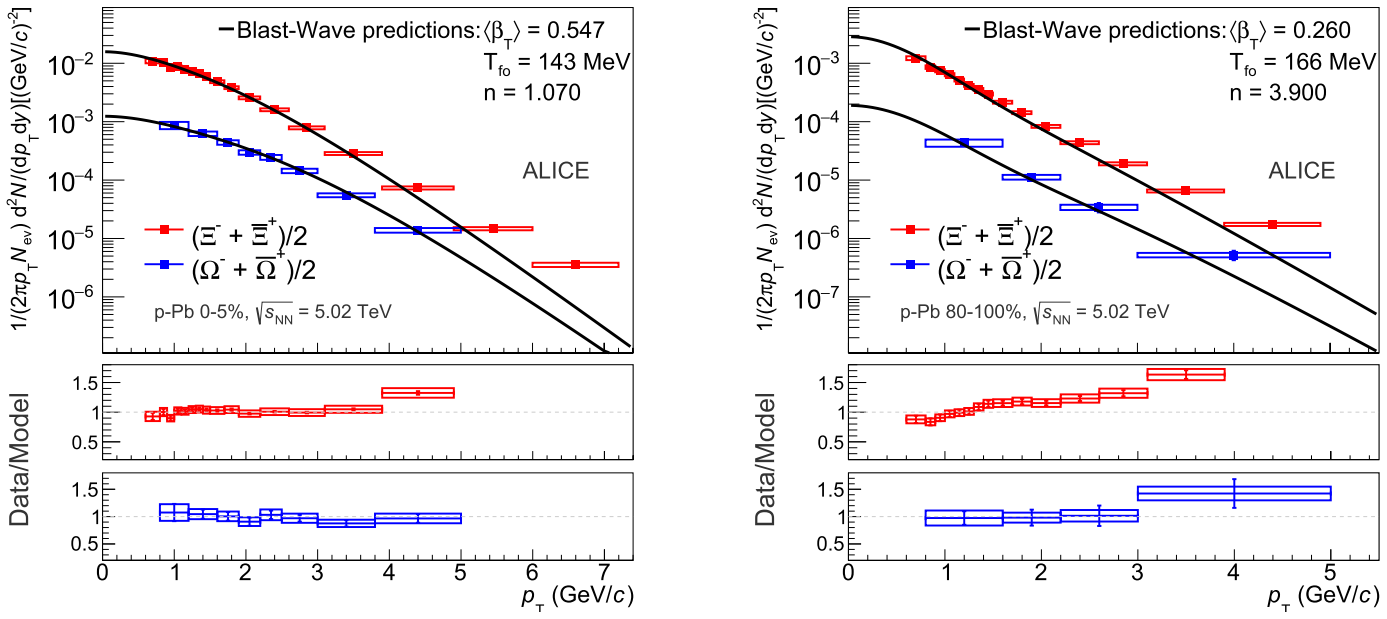

Fig. 3. (Colour online.) $(\Xi^- + \overline{\Xi}^+)/2$ and $(\Omega^- + \overline{\Omega}^+)/2$ p_{T} spectra in the 0–5% (left) and 80–100% (right) multiplicity classes compared to predictions from the BG–BW model (upper panels) with the ratios on a linear scale (lower panels). The parameters are based on simultaneous fits to lighter hadrons [23]. See text for details.

Table 3
The mid-rapidity $\langle \mathrm{d}N_{\mathrm{ch}}/\mathrm{d}\eta \rangle$ values for each of the 7 multiplicity classes and the $\Xi^- + \overline{\Xi}^+$ and $\Omega^- + \overline{\Omega}^+$ integrated yields per unit rapidity normalised to the visible cross section. The statistical uncertainty on the yields is followed by the systematic uncertainty.

Event class	$\langle \mathrm{d}N_{\mathrm{ch}}/\mathrm{d}\eta \rangle$ $\lvert\eta_{\mathrm{lab}}\rvert < 0.5$	$\mathrm{dN/dy}(\Xi^- + \overline{\Xi}^+)$	$\mathrm{dN/dy}(\Omega^- + \overline{\Omega}^+)$
0–5%	45 ± 1	$0.2354 \pm 0.0020 \pm 0.0161$	$0.0260 \pm 0.0011 \pm 0.0034$
5–10%	36.2 ± 0.8	$0.1861 \pm 0.0016 \pm 0.0138$	$0.0215 \pm 0.0008 \pm 0.0029$
10–20%	30.5 ± 0.7	$0.1500 \pm 0.0010 \pm 0.0112$	$0.0167 \pm 0.0006 \pm 0.0022$
20–40%	23.2 ± 0.5	$0.1100 \pm 0.0006 \pm 0.0085$	$0.0120 \pm 0.0005 \pm 0.0016$
40–60%	16.1 ± 0.4	$0.0726 \pm 0.0006 \pm 0.0065$	$0.0072 \pm 0.0003 \pm 0.0010$
60–80%	9.8 ± 0.24	$0.0398 \pm 0.0004 \pm 0.0031$	$0.0042 \pm 0.0002 \pm 0.0006$
80–100%	4.3 ± 0.1	$0.0143 \pm 0.0003 \pm 0.0015$	$0.0013 \pm 0.0003 \pm 0.0003$

Blast-Wave predictions become progressively worse. The comparison between lowest and highest multiplicity cases can be seen in Fig. 3, where their respective ratios to the model predictions are shown in the lower panels. These observations indicate that common kinetic freeze-out conditions are able to better describe the spectra in high multiplicity p–Pb collisions.

The multi-strange baryon spectra in central Pb–Pb collisions [10] have also been investigated in a common freeze-out scenario [17,18] and similar studies were performed for Au–Au collisions [19]. In contrast to high multiplicity p–Pb collisions, where all stable and long-lived hadron spectra are compatible with a single set of kinetic freeze-out conditions (the temperature $\mathrm{T_{fo}}$ and the mean transverse flow velocity $\langle \beta_{\mathrm{T}} \rangle$), multi-strange particles in central heavy-ion collisions seem to experience less transverse flow and may freeze out earlier in the evolution of the system when compared to most of the other hadrons.

3.3. Hyperon to pion ratios

The measured integrated yields in the seven multiplicity classes are given in Table 3. To study the relative production of strangeness and compare it with results in pp and Pb–Pb collisions, the yield ratios to pions were calculated as a function of charged particle multiplicity. Both the $(\Xi^- + \overline{\Xi}^+)/(\pi^+ + \pi^-)$ and $(\Omega^- + \overline{\Omega}^+)/(\pi^+ + \pi^-)$ ratios are observed to increase as a function of multiplicity, as seen in Fig. 4. The relative increase is more pronounced for the Ω^- and $\overline{\Omega}^+$ than for Ξ^- and $\overline{\Xi}^+$, being approximately 100% for the former and 60% for the latter. These relative increases are larger than the 30% increase observed for the Λ/π ratio [23], indicating that strangeness content may control the rate of increase with multiplicity.

These ratios are further compared to measurements performed in the pp [25,34] and Pb–Pb [10] collision systems. The $(\Xi^- + \overline{\Xi}^+)/(\pi^+ + \pi^-)$ ratio for the highest p–Pb multiplicity is compatible with the Pb–Pb measurements in the Pb–Pb 0–60% centrality range and the $(\Omega^- + \overline{\Omega}^+)/(\pi^+ + \pi^-)$ reaches a value slightly below its Pb–Pb equivalent in this centrality range, although the error bars still overlap. It is also noteworthy that the values obtained for the p–Pb 80–100% multiplicity event class are similar to the ones measured in minimum bias pp collisions.

Finally, the hyperon to pion ratios can also be compared with the values in the Grand Canonical (GC) limit obtained from global fits to Pb–Pb data. Two different implementations of the thermal model are shown in Fig. 4, where the dashed lines represent the values from the THERMUS 2.3 model [36] and the solid lines represent predictions from the GSI-Heidelberg model [35]. Both models provide values that are consistent with the most central Pb–Pb measurements.

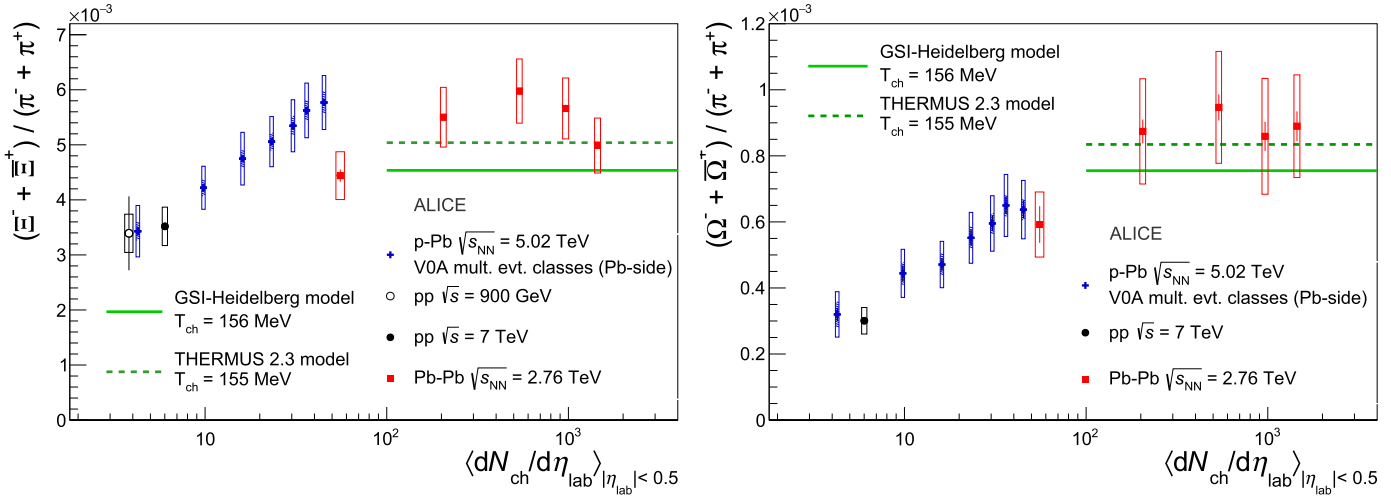

Fig. 4. (Colour online.) $(\Xi^- + \overline{\Xi}^+)/(\pi^+ + \pi^-)$ (left) and $(\Omega^- + \overline{\Omega}^+)/(\pi^+ + \pi^-)$ (right) ratios as a function of $\langle dN_{ch}/d\eta \rangle$ for all three colliding systems. The ratios for the seven multiplicity classes in p–Pb data lie between the Minimum Bias pp ($\sqrt{s} = 900$ GeV [32,33] and $\sqrt{s} = 7$ TeV [25,34]) and peripheral Pb–Pb results. The Pb–Pb points [10] represent, from left to right, the 60–80%, 40–60%, 20–40% and 10–20% and 0–10% centrality classes. The chemical equilibrium predictions by the GSI-Heidelberg [35] and the THERMUS 2.3 [36] models are represented by the horizontal lines.

In small multiplicity environments such as those produced in p–Pb collisions, a grand canonical statistical description may not be appropriate. Instead, local conservation laws might play an important role. The evolution of hyperon to pion ratios in terms of the event multiplicity can be calculated with a Strangeness Canonical (SC) model implemented in THERMUS [36]. This model applies a local conservation law to the strangeness quantum number within a correlation volume V_c while treating the baryon and charge quantum numbers grand-canonically within the fireball volume V. This implies a decrease of the strangeness yields with respect to the pion yields with a shrinking system size. To model this canonical suppression effect as a function of pion rapidity density, yield calculations were repeated for varying system sizes. Strangeness conservation was imposed within the size of the fireball ($V_c = V$), and the strangeness saturation parameter γ_S was fixed to 1, thus changes in the hadron to pion ratios were due to the variations of the restraints on the system size only. The chemical potentials (μ) of the conserved strangeness, baryon and electric charge quantum numbers were set to zero. The obtained suppression curves for Λ, Ξ and Ω are shown in Fig. 5 for a temperature of 155 MeV, the value extracted from a GC global fit to high multiplicity Pb–Pb data, with a variation of $\pm$10 MeV (solid lines). Both the data and model points were normalised to the high multiplicity limit. For the data, this limit is the mean hyperon to pion ratio in the 0–60% most central Pb–Pb events, whereas for the model it corresponds to the GC limit. The theoretical curves for strangeness suppression computed with THERMUS are in qualitative agreement with the effect observed in the data.

4. Conclusions

In summary, a measurement of the p_T spectra of Ξ^-, $\overline{\Xi}^+$, Ω^- and $\overline{\Omega}^+$ for seven multiplicity classes in p–Pb collisions at $\sqrt{s_{NN}} = 5.02$ TeV at the LHC has been presented. These measurements represent an important contribution to the understanding of strangeness production, as hyperon production rates are now measured at LHC energies over a large range in charged–particle multiplicity, from pp to central Pb–Pb collisions.

The multi-strange baryon spectra exhibit a progressive flattening with increasing multiplicity suggesting the presence of radial flow. A comparison with the Boltzmann–Gibbs Blast-Wave model indicates a common kinetic freeze-out with lighter hadrons in the highest multiplicity p–Pb collisions. This is in contrast to higher multiplicity heavy-ion collisions where there is an indication for an earlier freeze-out of these particles.

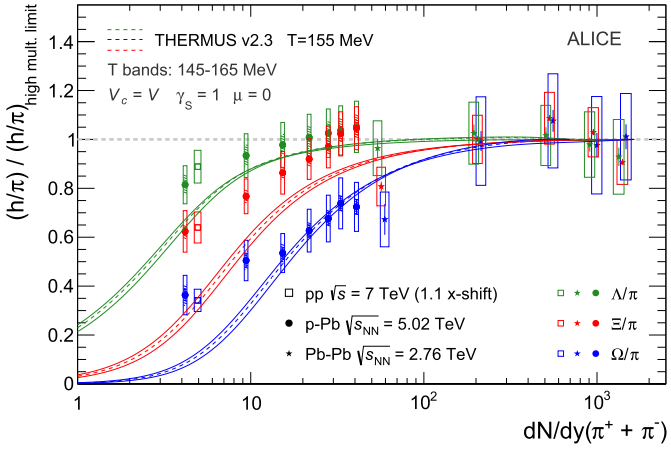

Fig. 5. (Colour online.) Hyperon to pion ratios as a function of pion yields for pp, p–Pb and Pb–Pb colliding systems compared to the THERMUS [36] strangeness suppression model prediction, in which only the system size is varied. The h/π are the ratios of the particle and antiparticle sums, except for the $2\Lambda/(\pi^- + \pi^+)$ data points in pp [33], p–Pb [23] and Pb–Pb [37]. All values are normalised to the high multiplicity limit, which is given by the mean of the 0–60% highest multiplicity Pb–Pb measurements for the data and by the GC limit for the model.

For the first time, the lifting of strangeness suppression with system size has been observed with measurements in a single collision system. Hyperon to pion ratios are shown to increase with multiplicity in p–Pb collisions from the values measured in pp to those observed in Pb–Pb. The rate of increase is more pronounced for particles with higher strangeness content. Comparing these results to the trends observed in statistical hadronisation models that conserve strangeness across the created system indicates that the behaviour is qualitatively consistent with the lifting of canonical suppression with increasing multiplicity.

Acknowledgements

The ALICE Collaboration would like to thank all its engineers and technicians for their invaluable contributions to the construction of the experiment and the CERN accelerator teams for the outstanding performance of the LHC complex. The ALICE Collaboration gratefully acknowledges the resources and support provided by all Grid centres and the Worldwide LHC Computing Grid (WLCG) collaboration. The ALICE Collaboration acknowledges the following funding agencies for their support in building and running the ALICE detector: State Committee of Science, World Federation of Scientists (WFS) and Swiss Fonds Kidagan, Armenia; Conselho Nacional de Desenvolvimento Científico e Tecnológico (CNPq), Financiadora de Estudos e Projetos (FINEP), Fundação de Amparo à Pesquisa do Estado de São Paulo (FAPESP); National Natural Science Foundation of China (NSFC), the Chinese Ministry of Education (CMOE) and the Ministry of Science and Technology of China (MSTC); Ministry of Education and Youth of the Czech Republic; Danish Natural Science Research Council, the Carlsberg Foundation and the Danish National Research Foundation; The European Research Council under the European Community's Seventh Framework Programme; Helsinki Institute of Physics and the Academy of Finland; French CNRS-IN2P3, the 'Region Pays de Loire', 'Region Alsace', 'Region Auvergne' and CEA, France; German Bundesministerium fur Bildung, Wissenschaft, Forschung und Technologie (BMBF) and the Helmholtz Association; General Secretariat for Research and Technology, Ministry of Development, Greece; National Research, Development and Innovation Office (NKFIH), Hungary; Department of Atomic Energy and Department of Science and Technology of the Government of India; Istituto Nazionale di Fisica Nucleare (INFN) and Centro Fermi – Museo Storico della Fisica e Centro Studi e Ricerche "Enrico Fermi", Italy; Japan Society for the Promotion of Science (JSPS) KAKENHI and MEXT, Japan; Joint Institute for Nuclear Research, Dubna; National Research Foundation of Korea (NRF); Consejo Nacional de Cienca y Tecnologia (CONACYT), Direccion General de Asuntos del Personal Academico (DGAPA), México, Amerique Latine Formation academique – European Commission (ALFA-EC) and the EPLANET Program (European Particle Physics Latin American Network); Stichting voor Fundamenteel Onderzoek der Materie (FOM) and the Nederlandse Organisatie voor Wetenschappelijk Onderzoek (NWO), Netherlands; Research Council of Norway (NFR); National Science Centre, Poland; Ministry of National Education/Institute for Atomic Physics and National Council of Scientific Research in Higher Education (CNCSI–UEFISCDI), Romania; Ministry of Education and Science of Russian Federation, Russian Academy of Sciences, Russian Federal Agency of Atomic Energy, Russian Federal Agency for Science and Innovation and The Russian Foundation for Basic Research; Ministry of Education of Slovakia; Department of Science and Technology, Republic of South Africa, South Africa; Centro de Investigaciones Energeticas, Medioambientales y Tecnologicas (CIEMAT), E-Infrastructure shared between Europe and Latin America (EELA), Ministerio de Economía y Competitividad (MINECO) of Spain, Xunta de Galicia (Consellería de Educación), Centro de Aplicaciones Tecnológicas y Desarrollo Nuclear (CEADEN), Cubaenergía, Cuba, and IAEA (International Atomic Energy Agency); Swedish Research Council (VR) and Knut & Alice Wallenberg Foundation (KAW); Ukraine Ministry of Education and Science; United Kingdom Science and Technology Facilities Council (STFC); The United States Department of Energy, the United States National Science Foundation, the State of Texas, and the State of Ohio; Ministry of Science, Education and Sports of Croatia and Unity through Knowledge Fund, Croatia; Council of Scientific and Industrial Research (CSIR), New Delhi, India; Pontificia Universidad Católica del Perú.

References

[1] J. Rafelski, B. Müller, Strangeness production in the quark–gluon plasma, Phys. Rev. Lett. 48 (1982) 1066–1069, http://link.aps.org/doi/10.1103/PhysRevLett.48.1066, Phys. Rev. Lett. 56 (1986) 2334 (Erratum).

[2] WA97 Collaboration, E. Andersen, et al., Enhancement of central Λ, Ξ and Ω yields in Pb–Pb collisions at 158 A GeV/c, Phys. Lett. B 433 (1998) 209–216, http://www.sciencedirect.com/science/article/pii/S0370269398006893.

[3] WA97 Collaboration, E. Andersen, et al., Strangeness enhancement at mid-rapidity in Pb–Pb collisions at 158 A GeV/c, Phys. Lett. B 449 (1999) 401–406, http://www.sciencedirect.com/science/article/pii/S0370269399001409.

[4] NA49 Collaboration, S. Afanasiev, et al., Ξ^- and $\overline{\Xi}^+$ production in central Pb+Pb collisions at 158 GeV/c per nucleon, Phys. Lett. B 538 (2002) 275–281, http://www.sciencedirect.com/science/article/pii/S0370269302019706.

[5] NA57 Collaboration, F. Antinori, et al., Energy dependence of hyperon production in nucleus–nucleus collisions at SPS, Phys. Lett. B 595 (2004) 68–74, http://www.sciencedirect.com/science/article/pii/S0370269304007725.

[6] NA49 Collaboration, T. Anticic, et al., Λ and $\overline{\Lambda}$ production in central Pb–Pb collisions at 40, 80, and 158A GeV, Phys. Rev. Lett. 93 (2004) 022302, http://link.aps.org/doi/10.1103/PhysRevLett.93.022302.

[7] STAR Collaboration, J. Adams, et al., Multistrange baryon production in Au–Au collisions at $\sqrt{s_{NN}} = 130$ GeV, Phys. Rev. Lett. 92 (2004) 182301, http://link.aps.org/doi/10.1103/PhysRevLett.92.182301.

[8] STAR Collaboration, J. Adams, et al., Scaling properties of hyperon production in Au + Au collisions at $\sqrt{s_{NN}} = 200$ GeV, Phys. Rev. Lett. 98 (2007) 062301, http://link.aps.org/doi/10.1103/PhysRevLett.98.062301.

[9] STAR Collaboration, B.I. Abelev, et al., Enhanced strange baryon production in Au+Au collisions compared to $p+p$ at $\sqrt{s_{NN}} = 200$ GeV, Phys. Rev. C 77 (2008) 044908, http://link.aps.org/doi/10.1103/PhysRevC.77.044908.

[10] ALICE Collaboration, B. Abelev, et al., Multi-strange baryon production at mid-rapidity in Pb–Pb collisions at $\sqrt{s_{NN}} = 2.76$ TeV, Phys. Lett. B 728 (2014) 216–227, http://www.sciencedirect.com/science/article/pii/S0370269313009544.

[11] K. Redlich, A. Tounsi, Strangeness enhancement and energy dependence in heavy ion collisions, Eur. Phys. J. C 24 (2002) 589–594, http://link.springer.com/article/10.1007/s10052-002-0983-1.

[12] I. Kraus, J. Cleymans, H. Oeschler, K. Redlich, Particle production in p–p collisions and predictions for $\sqrt{s} = 14$ TeV at the CERN Large Hadron Collider (LHC), Phys. Rev. C 79 (2009) 014901, http://link.aps.org/doi/10.1103/PhysRevC.79.014901.

[13] F. Becattini, J. Manninen, Strangeness production from SPS to LHC, J. Phys. G, Nucl. Part. Phys. 35 (2008) 104013, http://stacks.iop.org/0954-3899/35/i=10/a=104013.

[14] J. Aichelin, K. Werner, Centrality dependence of strangeness enhancement in ultrarelativistic heavy ion collisions: a core-corona effect, Phys. Rev. C 79 (2009) 064907, arXiv:0810.4465 [nucl-th], http://link.aps.org/doi/10.1103/PhysRevC.79.064907, Phys. Rev. C 81 (2010) 029902 (Erratum).

[15] STAR Collaboration, G. Agakishiev, et al., Strangeness enhancement in Cu–Cu and Au–Au collisions at $\sqrt{s_{NN}} = 200$ GeV, Phys. Rev. Lett. 108 (2012) 072301, http://link.aps.org/doi/10.1103/PhysRevLett.108.072301.

[16] E. Schnedermann, J. Sollfrank, U.W. Heinz, Thermal phenomenology of hadrons from 200A GeV S+S collisions, Phys. Rev. C 48 (1993) 2462–2475, arXiv:nucl-th/9307020, http://link.aps.org/doi/10.1103/PhysRevC.48.2462.

[17] V. Begun, W. Florkowski, M. Rybczynski, Transverse-momentum spectra of strange particles produced in Pb + Pb collisions at $\sqrt{s_{NN}} = 2.76$ TeV in the chemical nonequilibrium model, Phys. Rev. C 90 (2014) 054912, http://link.aps.org/doi/10.1103/PhysRevC.90.054912.

[18] I. Melo, B. Tomasik, Blast wave fits with resonances to p_t spectra from nuclear collisions at the LHC, in: 15th International Conference on Strangeness in Quark Matter (SQM 2015) Dubna, Moscow region, Russia, July 6–11, 2015, 2015, arXiv:1509.05383 [nucl-th].

[19] STAR Collaboration, J. Adams, et al., Experimental and theoretical challenges in the search for the quark–gluon plasma: the STAR Collaboration's critical assessment of the evidence from RHIC collisions, Nucl. Phys. A 757 (2005) 102–183, arXiv:nucl-ex/0501009, http://www.sciencedirect.com/science/article/pii/S0375947405005294.

[20] ALICE Collaboration, The ALICE experiment at the CERN LHC, J. Instrum. 3 (2008) S08002, http://stacks.iop.org/1748-0221/3/i=08/a=S08002.

[21] ALICE Collaboration, Performance of the ALICE VZERO system, J. Instrum. 8 (2013) P10016, http://stacks.iop.org/1748-0221/8/i=10/a=P10016.

[22] ALICE Collaboration, B. Abelev, et al., Pseudorapidity density of charged particles in p + Pb collisions at $\sqrt{s_{NN}} = 5.02$ TeV, Phys. Rev. Lett. 110 (2013) 032301, http://link.aps.org/doi/10.1103/PhysRevLett.110.032301.

[23] ALICE Collaboration, J. Adam, et al., Multiplicity dependence of pion, kaon, proton and lambda production in p–Pb collisions at $\sqrt{s_{NN}} = 5.02$ TeV, Phys. Lett. B 728 (2014) 25–38, http://www.sciencedirect.com/science/article/pii/S0370269313009234.

[24] K.A. Olive, et al., Particle data group, Chin. Phys. C 38 (2014) 090001, http://stacks.iop.org/1674-1137/38/i=9/a=090001.
[25] ALICE Collaboration, B. Abelev, et al., Multi-strange baryon production in pp collisions at $\sqrt{s} = 7$ TeV with ALICE, Phys. Lett. B 712 (2012) 309–318, http://www.sciencedirect.com/science/article/pii/S037026931200528X.
[26] ALICE Collaboration, Performance of the ALICE experiment at the CERN LHC, Int. J. Mod. Phys. A 29 (2014) 1430044, http://www.worldscientific.com/doi/abs/10.1142/S0217751X14300440.
[27] S. Roesler, R. Engel, J. Ranft, The Monte Carlo event generator DPMJET-III, in: A. Kling, F. Barão, M. Nakagawa, L. Távora, P. Vaz (Eds.), Advanced Monte Carlo for Radiation Physics, Particle Transport Simulation and Applications, Springer, Berlin, Heidelberg, 2001, pp. 1033–1038, arXiv:hep-ph/0012252.
[28] R. Brun, F. Bruyant, F. Carminati, S. Giani, M. Maire, A. McPherson, G. Patrick, L. Urban, Geant detector description and simulation tool, CERN Program Library Long Writeup (1994).
[29] C. Tsallis, Possible generalization of Boltzmann–Gibbs statistics, J. Stat. Phys. 52 (1988) 479–487.
[30] T. Sjostrand, S. Mrenna, P.Z. Skands, PYTHIA 6.4 physics and manual, J. High Energy Phys. 05 (2006) 026, arXiv:hep-ph/0603175.
[31] A. Ortiz Velasquez, P. Christiansen, E. Cuautle Flores, I.A. Maldonado Cervantes, G. Paić, Color reconnection and flowlike patterns in *pp* collisions, Phys. Rev. Lett. 111 (2013) 042001, http://link.aps.org/doi/10.1103/PhysRevLett.111.042001.
[32] ALICE Collaboration, K. Aamodt, et al., Production of pions, kaons and protons in pp collisions at $\sqrt{s} = 900$ GeV with ALICE at the LHC, Eur. Phys. J. C 71 (2011) 1655, http://dx.doi.org/10.1140/epjc/s10052-011-1655-9.
[33] ALICE Collaboration, K. Aamodt, et al., Strange particle production in proton–proton collisions at $\sqrt{s} = 0.9$ TeV with ALICE at the LHC, Eur. Phys. J. C 71 (2011) 1594, http://dx.doi.org/10.1140/epjc/s10052-011-1594-5.
[34] ALICE Collaboration, J. Adam, et al., Measurement of pion, kaon and proton production in proton–proton collisions at $\sqrt{s} = 7$ TeV, Eur. Phys. J. C 75 (2015) 226, http://dx.doi.org/10.1140/epjc/s10052-015-3422-9.
[35] A. Andronic, P. Braun-Munzinger, J. Stachel, Thermal hadron production in relativistic nuclear collisions: the hadron mass spectrum, the horn, and the QCD phase transition, Phys. Lett. B 673 (2009) 142–145, http://www.sciencedirect.com/science/article/pii/S0370269309001609.
[36] S. Wheaton, J. Cleymans, M. Hauer, THERMUS — a thermal model package for ROOT, Comput. Phys. Commun. 180 (2009) 84–106, http://www.sciencedirect.com/science/article/pii/S0010465508002750.
[37] ALICE Collaboration, B.B. Abelev, et al., K^0_S and Λ production in Pb–Pb collisions at $\sqrt{s_{NN}} = 2.76$ TeV, Phys. Rev. Lett. 111 (2013) 222301, arXiv:1307.5530 [nucl-ex].

ALICE Collaboration

J. Adam [40], D. Adamová [84], M.M. Aggarwal [88], G. Aglieri Rinella [36], M. Agnello [110], N. Agrawal [48], Z. Ahammed [132], S. Ahmad [19], S.U. Ahn [68], S. Aiola [136], A. Akindinov [58], S.N. Alam [132], D. Aleksandrov [80], B. Alessandro [110], D. Alexandre [101], R. Alfaro Molina [64], A. Alici [12,104], A. Alkin [3], J.R.M. Almaraz [119], J. Alme [38], T. Alt [43], S. Altinpinar [18], I. Altsybeev [131], C. Alves Garcia Prado [120], C. Andrei [78], A. Andronic [97], V. Anguelov [94], J. Anielski [54], T. Antičić [98], F. Antinori [107], P. Antonioli [104], L. Aphecetche [113], H. Appelshäuser [53], S. Arcelli [28], R. Arnaldi [110], O.W. Arnold [37,93], I.C. Arsene [22], M. Arslandok [53], B. Audurier [113], A. Augustinus [36], R. Averbeck [97], M.D. Azmi [19], A. Badalà [106], Y.W. Baek [67], S. Bagnasco [110], R. Bailhache [53], R. Bala [91], S. Balasubramanian [136], A. Baldisseri [15], R.C. Baral [61], A.M. Barbano [27], R. Barbera [29], F. Barile [33], G.G. Barnaföldi [135], L.S. Barnby [101], V. Barret [70], P. Bartalini [7], K. Barth [36], J. Bartke [117], E. Bartsch [53], M. Basile [28], N. Bastid [70], S. Basu [132], B. Bathen [54], G. Batigne [113], A. Batista Camejo [70], B. Batyunya [66], P.C. Batzing [22], I.G. Bearden [81], H. Beck [53], C. Bedda [110], N.K. Behera [50], I. Belikov [55], F. Bellini [28], H. Bello Martinez [2], R. Bellwied [122], R. Belmont [134], E. Belmont-Moreno [64], V. Belyaev [75], P. Benacek [84], G. Bencedi [135], S. Beole [27], I. Berceanu [78], A. Bercuci [78], Y. Berdnikov [86], D. Berenyi [135], R.A. Bertens [57], D. Berzano [36], L. Betev [36], A. Bhasin [91], I.R. Bhat [91], A.K. Bhati [88], B. Bhattacharjee [45], J. Bhom [128], L. Bianchi [122], N. Bianchi [72], C. Bianchin [134,57], J. Bielčík [40], J. Bielčíková [84], A. Bilandzic [81,37,93], G. Biro [135], R. Biswas [4], S. Biswas [79], S. Bjelogrlic [57], J.T. Blair [118], D. Blau [80], C. Blume [53], F. Bock [74,94], A. Bogdanov [75], H. Bøggild [81], L. Boldizsár [135], M. Bombara [41], J. Book [53], H. Borel [15], A. Borissov [96], M. Borri [83,124], F. Bossú [65], E. Botta [27], C. Bourjau [81], P. Braun-Munzinger [97], M. Bregant [120], T. Breitner [52], T.A. Broker [53], T.A. Browning [95], M. Broz [40], E.J. Brucken [46], E. Bruna [110], G.E. Bruno [33], D. Budnikov [99], H. Buesching [53], S. Bufalino [36,27], P. Buncic [36], O. Busch [94,128], Z. Buthelezi [65], J.B. Butt [16], J.T. Buxton [20], D. Caffarri [36], X. Cai [7], H. Caines [136], L. Calero Diaz [72], A. Caliva [57], E. Calvo Villar [102], P. Camerini [26], F. Carena [36], W. Carena [36], F. Carnesecchi [28], J. Castillo Castellanos [15], A.J. Castro [125], E.A.R. Casula [25], C. Ceballos Sanchez [9], P. Cerello [110], J. Cerkala [115], B. Chang [123], S. Chapeland [36], M. Chartier [124], J.L. Charvet [15], S. Chattopadhyay [132], S. Chattopadhyay [100], A. Chauvin [93,37], V. Chelnokov [3], M. Cherney [87], C. Cheshkov [130], B. Cheynis [130], V. Chibante Barroso [36], D.D. Chinellato [121], S. Cho [50], P. Chochula [36], K. Choi [96], M. Chojnacki [81], S. Choudhury [132], P. Christakoglou [82], C.H. Christensen [81], P. Christiansen [34], T. Chujo [128], S.U. Chung [96], C. Cicalo [105], L. Cifarelli [12,28], F. Cindolo [104], J. Cleymans [90], F. Colamaria [33], D. Colella [59,36], A. Collu [74,25], M. Colocci [28], G. Conesa Balbastre [71], Z. Conesa del Valle [51], M.E. Connors [136,ii], J.G. Contreras [40], T.M. Cormier [85], Y. Corrales Morales [110], I. Cortés Maldonado [2], P. Cortese [32], M.R. Cosentino [120], F. Costa [36], P. Crochet [70], R. Cruz Albino [11], E. Cuautle [63], L. Cunqueiro [54,36], T. Dahms [93,37], A. Dainese [107], A. Danu [62], D. Das [100], I. Das [100,51], S. Das [4], A. Dash [121,79], S. Dash [48], S. De [120], A. De Caro [12,31], G. de Cataldo [103], C. de Conti [120], J. de Cuveland [43], A. De Falco [25], D. De Gruttola [12,31], N. De Marco [110], S. De Pasquale [31], A. Deisting [97,94], A. Deloff [77], E. Dénes [135,i], C. Deplano [82], P. Dhankher [48], D. Di Bari [33], A. Di Mauro [36], P. Di Nezza [72], M.A. Diaz Corchero [10], T. Dietel [90], P. Dillenseger [53], R. Divià [36], Ø. Djuvsland [18], A. Dobrin [57,82],

D. Domenicis Gimenez [120], B. Dönigus [53], O. Dordic [22], T. Drozhzhova [53], A.K. Dubey [132], A. Dubla [57], L. Ducroux [130], P. Dupieux [70], R.J. Ehlers [136], D. Elia [103], E. Endress [102], H. Engel [52], E. Epple [136], B. Erazmus [113], I. Erdemir [53], F. Erhardt [129], B. Espagnon [51], M. Estienne [113], S. Esumi [128], J. Eum [96], D. Evans [101], S. Evdokimov [111], G. Eyyubova [40], L. Fabbietti [93,37], D. Fabris [107], J. Faivre [71], A. Fantoni [72], M. Fasel [74], L. Feldkamp [54], A. Feliciello [110], G. Feofilov [131], J. Ferencei [84], A. Fernández Téllez [2], E.G. Ferreiro [17], A. Ferretti [27], A. Festanti [30], V.J.G. Feuillard [15,70], J. Figiel [117], M.A.S. Figueredo [124,120], S. Filchagin [99], D. Finogeev [56], F.M. Fionda [25], E.M. Fiore [33], M.G. Fleck [94], M. Floris [36], S. Foertsch [65], P. Foka [97], S. Fokin [80], E. Fragiacomo [109], A. Francescon [36,30], U. Frankenfeld [97], G.G. Fronze [27], U. Fuchs [36], C. Furget [71], A. Furs [56], M. Fusco Girard [31], J.J. Gaardhøje [81], M. Gagliardi [27], A.M. Gago [102], M. Gallio [27], D.R. Gangadharan [74], P. Ganoti [89], C. Gao [7], C. Garabatos [97], E. Garcia-Solis [13], C. Gargiulo [36], P. Gasik [93,37], E.F. Gauger [118], M. Germain [113], A. Gheata [36], M. Gheata [36,62], P. Ghosh [132], S.K. Ghosh [4], P. Gianotti [72], P. Giubellino [110,36], P. Giubilato [30], E. Gladysz-Dziadus [117], P. Glässel [94], D.M. Goméz Coral [64], A. Gomez Ramirez [52], V. Gonzalez [10], P. González-Zamora [10], S. Gorbunov [43], L. Görlich [117], S. Gotovac [116], V. Grabski [64], O.A. Grachov [136], L.K. Graczykowski [133], K.L. Graham [101], A. Grelli [57], A. Grigoras [36], C. Grigoras [36], V. Grigoriev [75], A. Grigoryan [1], S. Grigoryan [66], B. Grinyov [3], N. Grion [109], J.M. Gronefeld [97], J.F. Grosse-Oetringhaus [36], J.-Y. Grossiord [130], R. Grosso [97], F. Guber [56], R. Guernane [71], B. Guerzoni [28], K. Gulbrandsen [81], T. Gunji [127], A. Gupta [91], R. Gupta [91], R. Haake [54], Ø. Haaland [18], C. Hadjidakis [51], M. Haiduc [62], H. Hamagaki [127], G. Hamar [135], J.C. Hamon [55], J.W. Harris [136], A. Harton [13], D. Hatzifotiadou [104], S. Hayashi [127], S.T. Heckel [53], H. Helstrup [38], A. Herghelegiu [78], G. Herrera Corral [11], B.A. Hess [35], K.F. Hetland [38], H. Hillemanns [36], B. Hippolyte [55], D. Horak [40], R. Hosokawa [128], P. Hristov [36], M. Huang [18], T.J. Humanic [20], N. Hussain [45], T. Hussain [19], D. Hutter [43], D.S. Hwang [21], R. Ilkaev [99], M. Inaba [128], E. Incani [25], M. Ippolitov [75,80], M. Irfan [19], M. Ivanov [97], V. Ivanov [86], V. Izucheev [111], N. Jacazio [28], P.M. Jacobs [74], M.B. Jadhav [48], S. Jadlovska [115], J. Jadlovsky [115,59], C. Jahnke [120], M.J. Jakubowska [133], H.J. Jang [68], M.A. Janik [133], P.H.S.Y. Jayarathna [122], C. Jena [30], S. Jena [122], R.T. Jimenez Bustamante [97], P.G. Jones [101], H. Jung [44], A. Jusko [101], P. Kalinak [59], A. Kalweit [36], J. Kamin [53], J.H. Kang [137], V. Kaplin [75], S. Kar [132], A. Karasu Uysal [69], O. Karavichev [56], T. Karavicheva [56], L. Karayan [97,94], E. Karpechev [56], U. Kebschull [52], R. Keidel [138], D.L.D. Keijdener [57], M. Keil [36], M. Mohisin Khan [19,iii], P. Khan [100], S.A. Khan [132], A. Khanzadeev [86], Y. Kharlov [111], B. Kileng [38], D.W. Kim [44], D.J. Kim [123], D. Kim [137], H. Kim [137], J.S. Kim [44], M. Kim [44], M. Kim [137], S. Kim [21], T. Kim [137], S. Kirsch [43], I. Kisel [43], S. Kiselev [58], A. Kisiel [133], G. Kiss [135], J.L. Klay [6], C. Klein [53], J. Klein [36], C. Klein-Bösing [54], S. Klewin [94], A. Kluge [36], M.L. Knichel [94], A.G. Knospe [118], C. Kobdaj [114], M. Kofarago [36], T. Kollegger [97], A. Kolojvari [131], V. Kondratiev [131], N. Kondratyeva [75], E. Kondratyuk [111], A. Konevskikh [56], M. Kopcik [115], M. Kour [91], C. Kouzinopoulos [36], O. Kovalenko [77], V. Kovalenko [131], M. Kowalski [117], G. Koyithatta Meethaleveedu [48], I. Králik [59], A. Kravčáková [41], M. Kretz [43], M. Krivda [59,101], F. Krizek [84], E. Kryshen [86,36], M. Krzewicki [43], A.M. Kubera [20], V. Kučera [84], C. Kuhn [55], P.G. Kuijer [82], A. Kumar [91], J. Kumar [48], L. Kumar [88], S. Kumar [48], P. Kurashvili [77], A. Kurepin [56], A.B. Kurepin [56], A. Kuryakin [99], M.J. Kweon [50], Y. Kwon [137], S.L. La Pointe [110], P. La Rocca [29], P. Ladron de Guevara [11], C. Lagana Fernandes [120], I. Lakomov [36], R. Langoy [42], C. Lara [52], A. Lardeux [15], A. Lattuca [27], E. Laudi [36], R. Lea [26], L. Leardini [94], G.R. Lee [101], S. Lee [137], F. Lehas [82], R.C. Lemmon [83], V. Lenti [103], E. Leogrande [57], I. León Monzón [119], H. León Vargas [64], M. Leoncino [27], P. Lévai [135], S. Li [7,70], X. Li [14], J. Lien [42], R. Lietava [101], S. Lindal [22], V. Lindenstruth [43], C. Lippmann [97], M.A. Lisa [20], H.M. Ljunggren [34], D.F. Lodato [57], P.I. Loenne [18], V. Loginov [75], C. Loizides [74], X. Lopez [70], E. López Torres [9], A. Lowe [135], P. Luettig [53], M. Lunardon [30], G. Luparello [26], T.H. Lutz [136], A. Maevskaya [56], M. Mager [36], S. Mahajan [91], S.M. Mahmood [22], A. Maire [55], R.D. Majka [136], M. Malaev [86], I. Maldonado Cervantes [63], L. Malinina [66,iv], D. Mal'Kevich [58], P. Malzacher [97], A. Mamonov [99], V. Manko [80], F. Manso [70], V. Manzari [36,103], M. Marchisone [65,126,27], J. Mareš [60], G.V. Margagliotti [26], A. Margotti [104], J. Margutti [57], A. Marín [97], C. Markert [118], M. Marquard [53], N.A. Martin [97], J. Martin Blanco [113], P. Martinengo [36], M.I. Martínez [2], G. Martínez García [113], M. Martinez Pedreira [36], A. Mas [120], S. Masciocchi [97], M. Masera [27], A. Masoni [105], L. Massacrier [113], A. Mastroserio [33], A. Matyja [117], C. Mayer [36,117], J. Mazer [125], M.A. Mazzoni [108], D. Mcdonald [122], F. Meddi [24], Y. Melikyan [75], A. Menchaca-Rocha [64], E. Meninno [31], J. Mercado Pérez [94], M. Meres [39], Y. Miake [128], M.M. Mieskolainen [46], K. Mikhaylov [66,58], L. Milano [74,36], J. Milosevic [22], L.M. Minervini [103,23], A. Mischke [57], A.N. Mishra [49], D. Miśkowiec [97], J. Mitra [132], C.M. Mitu [62],

N. Mohammadi [57], B. Mohanty [79,132], L. Molnar [55,113], L. Montaño Zetina [11], E. Montes [10], D.A. Moreira De Godoy [54,113], L.A.P. Moreno [2], S. Moretto [30], A. Morreale [113], A. Morsch [36], V. Muccifora [72], E. Mudnic [116], D. Mühlheim [54], S. Muhuri [132], M. Mukherjee [132], J.D. Mulligan [136], M.G. Munhoz [120], R.H. Munzer [93,37], H. Murakami [127], S. Murray [65], L. Musa [36], J. Musinsky [59], B. Naik [48], R. Nair [77], B.K. Nandi [48], R. Nania [104], E. Nappi [103], M.U. Naru [16], H. Natal da Luz [120], C. Nattrass [125], S.R. Navarro [2], K. Nayak [79], R. Nayak [48], T.K. Nayak [132], S. Nazarenko [99], A. Nedosekin [58], L. Nellen [63], F. Ng [122], M. Nicassio [97], M. Niculescu [62], J. Niedziela [36], B.S. Nielsen [81], S. Nikolaev [80], S. Nikulin [80], V. Nikulin [86], F. Noferini [104,12], P. Nomokonov [66], G. Nooren [57], J.C.C. Noris [2], J. Norman [124], A. Nyanin [80], J. Nystrand [18], H. Oeschler [94], S. Oh [136], S.K. Oh [67], A. Ohlson [36], A. Okatan [69], T. Okubo [47], L. Olah [135], J. Oleniacz [133], A.C. Oliveira Da Silva [120], M.H. Oliver [136], J. Onderwaater [97], C. Oppedisano [110], R. Orava [46], A. Ortiz Velasquez [63], A. Oskarsson [34], J. Otwinowski [117], K. Oyama [94,76], M. Ozdemir [53], Y. Pachmayer [94], P. Pagano [31], G. Paić [63], S.K. Pal [132], J. Pan [134], A.K. Pandey [48], P. Papcun [115], V. Papikyan [1], G.S. Pappalardo [106], P. Pareek [49], W.J. Park [97], S. Parmar [88], A. Passfeld [54], V. Paticchio [103], R.N. Patra [132], B. Paul [100], H. Pei [7], T. Peitzmann [57], H. Pereira Da Costa [15], D. Peresunko [80,75], C.E. Pérez Lara [82], E. Perez Lezama [53], V. Peskov [53], Y. Pestov [5], V. Petráček [40], V. Petrov [111], M. Petrovici [78], C. Petta [29], S. Piano [109], M. Pikna [39], P. Pillot [113], L.O.D.L. Pimentel [81], O. Pinazza [36,104], L. Pinsky [122], D.B. Piyarathna [122], M. Płoskoń [74], M. Planinic [129], J. Pluta [133], S. Pochybova [135], P.L.M. Podesta-Lerma [119], M.G. Poghosyan [85,87], B. Polichtchouk [111], N. Poljak [129], W. Poonsawat [114], A. Pop [78], S. Porteboeuf-Houssais [70], J. Porter [74], J. Pospisil [84], S.K. Prasad [4], R. Preghenella [104,36], F. Prino [110], C.A. Pruneau [134], I. Pshenichnov [56], M. Puccio [27], G. Puddu [25], P. Pujahari [134], V. Punin [99], J. Putschke [134], H. Qvigstad [22], A. Rachevski [109], S. Raha [4], S. Rajput [91], J. Rak [123], A. Rakotozafindrabe [15], L. Ramello [32], F. Rami [55], R. Raniwala [92], S. Raniwala [92], S.S. Räsänen [46], B.T. Rascanu [53], D. Rathee [88], K.F. Read [125,85], K. Redlich [77], R.J. Reed [134], A. Rehman [18], P. Reichelt [53], F. Reidt [94,36], X. Ren [7], R. Renfordt [53], A.R. Reolon [72], A. Reshetin [56], J.-P. Revol [12], K. Reygers [94], V. Riabov [86], R.A. Ricci [73], T. Richert [34], M. Richter [22], P. Riedler [36], W. Riegler [36], F. Riggi [29], C. Ristea [62], E. Rocco [57], M. Rodríguez Cahuantzi [2,11], A. Rodriguez Manso [82], K. Røed [22], E. Rogochaya [66], D. Rohr [43], D. Röhrich [18], R. Romita [124], F. Ronchetti [72,36], L. Ronflette [113], P. Rosnet [70], A. Rossi [30,36], F. Roukoutakis [89], A. Roy [49], C. Roy [55], P. Roy [100], A.J. Rubio Montero [10], R. Rui [26], R. Russo [27], E. Ryabinkin [80], Y. Ryabov [86], A. Rybicki [117], S. Sadovsky [111], K. Šafařík [36], B. Sahlmuller [53], P. Sahoo [49], R. Sahoo [49], S. Sahoo [61], P.K. Sahu [61], J. Saini [132], S. Sakai [72], M.A. Saleh [134], J. Salzwedel [20], S. Sambyal [91], V. Samsonov [86], L. Šándor [59], A. Sandoval [64], M. Sano [128], D. Sarkar [132], P. Sarma [45], E. Scapparone [104], F. Scarlassara [30], C. Schiaua [78], R. Schicker [94], C. Schmidt [97], H.R. Schmidt [35], S. Schuchmann [53], J. Schukraft [36], M. Schulc [40], T. Schuster [136], Y. Schutz [36,113], K. Schwarz [97], K. Schweda [97], G. Scioli [28], E. Scomparin [110], R. Scott [125], M. Šefčík [41], J.E. Seger [87], Y. Sekiguchi [127], D. Sekihata [47], I. Selyuzhenkov [97], K. Senosi [65], S. Senyukov [3,36], E. Serradilla [10,64], A. Sevcenco [62], A. Shabanov [56], A. Shabetai [113], O. Shadura [3], R. Shahoyan [36], A. Shangaraev [111], A. Sharma [91], M. Sharma [91], M. Sharma [91], N. Sharma [125], K. Shigaki [47], K. Shtejer [9,27], Y. Sibiriak [80], S. Siddhanta [105], K.M. Sielewicz [36], T. Siemiarczuk [77], D. Silvermyr [34], C. Silvestre [71], G. Simatovic [129], G. Simonetti [36], R. Singaraju [132], R. Singh [79], S. Singha [132,79], V. Singhal [132], B.C. Sinha [132], T. Sinha [100], B. Sitar [39], M. Sitta [32], T.B. Skaali [22], M. Slupecki [123], N. Smirnov [136], R.J.M. Snellings [57], T.W. Snellman [123], C. Søgaard [34], J. Song [96], M. Song [137], Z. Song [7], F. Soramel [30], S. Sorensen [125], R.D. de Souza [121], F. Sozzi [97], M. Spacek [40], E. Spiriti [72], I. Sputowska [117], M. Spyropoulou-Stassinaki [89], J. Stachel [94], I. Stan [62], P. Stankus [85], G. Stefanek [77], E. Stenlund [34], G. Steyn [65], J.H. Stiller [94], D. Stocco [113], P. Strmen [39], A.A.P. Suaide [120], T. Sugitate [47], C. Suire [51], M. Suleymanov [16], M. Suljic [26,i], R. Sultanov [58], M. Šumbera [84], A. Szabo [39], A. Szanto de Toledo [120,i], I. Szarka [39], A. Szczepankiewicz [36], M. Szymanski [133], U. Tabassam [16], J. Takahashi [121], G.J. Tambave [18], N. Tanaka [128], M.A. Tangaro [33], M. Tarhini [51], M. Tariq [19], M.G. Tarzila [78], A. Tauro [36], G. Tejeda Muñoz [2], A. Telesca [36], K. Terasaki [127], C. Terrevoli [30], B. Teyssier [130], J. Thäder [74], D. Thomas [118], R. Tieulent [130], A.R. Timmins [122], A. Toia [53], S. Trogolo [27], G. Trombetta [33], V. Trubnikov [3], W.H. Trzaska [123], T. Tsuji [127], A. Tumkin [99], R. Turrisi [107], T.S. Tveter [22], K. Ullaland [18], A. Uras [130], G.L. Usai [25], A. Utrobicic [129], M. Vajzer [84], M. Vala [59], L. Valencia Palomo [70], S. Vallero [27], J. Van Der Maarel [57], J.W. Van Hoorne [36], M. van Leeuwen [57], T. Vanat [84], P. Vande Vyvre [36], D. Varga [135], A. Vargas [2], M. Vargyas [123], R. Varma [48], M. Vasileiou [89], A. Vasiliev [80], A. Vauthier [71], V. Vechernin [131], A.M. Veen [57], M. Veldhoen [57], A. Velure [18],

M. Venaruzzo [73], E. Vercellin [27], S. Vergara Limón [2], R. Vernet [8], M. Verweij [134], L. Vickovic [116], G. Viesti [30,i], J. Viinikainen [123], Z. Vilakazi [126], O. Villalobos Baillie [101], A. Villatoro Tello [2], A. Vinogradov [80], L. Vinogradov [131], Y. Vinogradov [99,i], T. Virgili [31], V. Vislavicius [34], Y.P. Viyogi [132], A. Vodopyanov [66], M.A. Völkl [94], K. Voloshin [58], S.A. Voloshin [134], G. Volpe [135], B. von Haller [36], I. Vorobyev [37,93], D. Vranic [97,36], J. Vrláková [41], B. Vulpescu [70], B. Wagner [18], J. Wagner [97], H. Wang [57], M. Wang [7,113], D. Watanabe [128], Y. Watanabe [127], M. Weber [36,112], S.G. Weber [97], D.F. Weiser [94], J.P. Wessels [54], U. Westerhoff [54], A.M. Whitehead [90], J. Wiechula [35], J. Wikne [22], M. Wilde [54], G. Wilk [77], J. Wilkinson [94], M.C.S. Williams [104], B. Windelband [94], M. Winn [94], C.G. Yaldo [134], H. Yang [57], P. Yang [7], S. Yano [47], C. Yasar [69], Z. Yin [7], H. Yokoyama [128], I.-K. Yoo [96], J.H. Yoon [50], V. Yurchenko [3], I. Yushmanov [80], A. Zaborowska [133], V. Zaccolo [81], A. Zaman [16], C. Zampolli [104], H.J.C. Zanoli [120], S. Zaporozhets [66], N. Zardoshti [101], A. Zarochentsev [131], P. Závada [60], N. Zaviyalov [99], H. Zbroszczyk [133], I.S. Zgura [62], M. Zhalov [86], H. Zhang [18], X. Zhang [74], Y. Zhang [7], C. Zhang [57], Z. Zhang [7], C. Zhao [22], N. Zhigareva [58], D. Zhou [7], Y. Zhou [81], Z. Zhou [18], H. Zhu [18], J. Zhu [113,7], A. Zichichi [28,12], A. Zimmermann [94], M.B. Zimmermann [54,36], G. Zinovjev [3], M. Zyzak [43]

[1] *A.I. Alikhanyan National Science Laboratory (Yerevan Physics Institute) Foundation, Yerevan, Armenia*
[2] *Benemérita Universidad Autónoma de Puebla, Puebla, Mexico*
[3] *Bogolyubov Institute for Theoretical Physics, Kiev, Ukraine*
[4] *Bose Institute, Department of Physics and Centre for Astroparticle Physics and Space Science (CAPSS), Kolkata, India*
[5] *Budker Institute for Nuclear Physics, Novosibirsk, Russia*
[6] *California Polytechnic State University, San Luis Obispo, CA, United States*
[7] *Central China Normal University, Wuhan, China*
[8] *Centre de Calcul de l'IN2P3, Villeurbanne, France*
[9] *Centro de Aplicaciones Tecnológicas y Desarrollo Nuclear (CEADEN), Havana, Cuba*
[10] *Centro de Investigaciones Energéticas Medioambientales y Tecnológicas (CIEMAT), Madrid, Spain*
[11] *Centro de Investigación y de Estudios Avanzados (CINVESTAV), Mexico City and Mérida, Mexico*
[12] *Centro Fermi – Museo Storico della Fisica e Centro Studi e Ricerche "Enrico Fermi", Rome, Italy*
[13] *Chicago State University, Chicago, IL, USA*
[14] *China Institute of Atomic Energy, Beijing, China*
[15] *Commissariat à l'Energie Atomique, IRFU, Saclay, France*
[16] *COMSATS Institute of Information Technology (CIIT), Islamabad, Pakistan*
[17] *Departamento de Física de Partículas and IGFAE, Universidad de Santiago de Compostela, Santiago de Compostela, Spain*
[18] *Department of Physics and Technology, University of Bergen, Bergen, Norway*
[19] *Department of Physics, Aligarh Muslim University, Aligarh, India*
[20] *Department of Physics, Ohio State University, Columbus, OH, United States*
[21] *Department of Physics, Sejong University, Seoul, South Korea*
[22] *Department of Physics, University of Oslo, Oslo, Norway*
[23] *Dipartimento di Elettrotecnica ed Elettronica del Politecnico, Bari, Italy*
[24] *Dipartimento di Fisica dell'Università 'La Sapienza' and Sezione INFN, Rome, Italy*
[25] *Dipartimento di Fisica dell'Università and Sezione INFN, Cagliari, Italy*
[26] *Dipartimento di Fisica dell'Università and Sezione INFN, Trieste, Italy*
[27] *Dipartimento di Fisica dell'Università and Sezione INFN, Turin, Italy*
[28] *Dipartimento di Fisica e Astronomia dell'Università and Sezione INFN, Bologna, Italy*
[29] *Dipartimento di Fisica e Astronomia dell'Università and Sezione INFN, Catania, Italy*
[30] *Dipartimento di Fisica e Astronomia dell'Università and Sezione INFN, Padova, Italy*
[31] *Dipartimento di Fisica 'E.R. Caianiello' dell'Università and Gruppo Collegato INFN, Salerno, Italy*
[32] *Dipartimento di Scienze e Innovazione Tecnologica dell'Università del Piemonte Orientale and Gruppo Collegato INFN, Alessandria, Italy*
[33] *Dipartimento Interateneo di Fisica 'M. Merlin' and Sezione INFN, Bari, Italy*
[34] *Division of Experimental High Energy Physics, University of Lund, Lund, Sweden*
[35] *Eberhard Karls Universität Tübingen, Tübingen, Germany*
[36] *European Organization for Nuclear Research (CERN), Geneva, Switzerland*
[37] *Excellence Cluster Universe, Technische Universität München, Munich, Germany*
[38] *Faculty of Engineering, Bergen University College, Bergen, Norway*
[39] *Faculty of Mathematics, Physics and Informatics, Comenius University, Bratislava, Slovakia*
[40] *Faculty of Nuclear Sciences and Physical Engineering, Czech Technical University in Prague, Prague, Czech Republic*
[41] *Faculty of Science, P.J. Šafárik University, Košice, Slovakia*
[42] *Faculty of Technology, Buskerud and Vestfold University College, Vestfold, Norway*
[43] *Frankfurt Institute for Advanced Studies, Johann Wolfgang Goethe-Universität Frankfurt, Frankfurt, Germany*
[44] *Gangneung-Wonju National University, Gangneung, South Korea*
[45] *Gauhati University, Department of Physics, Guwahati, India*
[46] *Helsinki Institute of Physics (HIP), Helsinki, Finland*
[47] *Hiroshima University, Hiroshima, Japan*
[48] *Indian Institute of Technology Bombay (IIT), Mumbai, India*
[49] *Indian Institute of Technology Indore, Indore (IITI), India*
[50] *Inha University, Incheon, South Korea*
[51] *Institut de Physique Nucléaire d'Orsay (IPNO), Université Paris-Sud, CNRS-IN2P3, Orsay, France*
[52] *Institut für Informatik, Johann Wolfgang Goethe-Universität Frankfurt, Frankfurt, Germany*
[53] *Institut für Kernphysik, Johann Wolfgang Goethe-Universität Frankfurt, Frankfurt, Germany*
[54] *Institut für Kernphysik, Westfälische Wilhelms-Universität Münster, Münster, Germany*
[55] *Institut Pluridisciplinaire Hubert Curien (IPHC), Université de Strasbourg, CNRS-IN2P3, Strasbourg, France*
[56] *Institute for Nuclear Research, Academy of Sciences, Moscow, Russia*
[57] *Institute for Subatomic Physics of Utrecht University, Utrecht, Netherlands*

[58] Institute for Theoretical and Experimental Physics, Moscow, Russia
[59] Institute of Experimental Physics, Slovak Academy of Sciences, Košice, Slovakia
[60] Institute of Physics, Academy of Sciences of the Czech Republic, Prague, Czech Republic
[61] Institute of Physics, Bhubaneswar, India
[62] Institute of Space Science (ISS), Bucharest, Romania
[63] Instituto de Ciencias Nucleares, Universidad Nacional Autónoma de México, Mexico City, Mexico
[64] Instituto de Física, Universidad Nacional Autónoma de México, Mexico City, Mexico
[65] iThemba LABS, National Research Foundation, Somerset West, South Africa
[66] Joint Institute for Nuclear Research (JINR), Dubna, Russia
[67] Konkuk University, Seoul, South Korea
[68] Korea Institute of Science and Technology Information, Daejeon, South Korea
[69] KTO Karatay University, Konya, Turkey
[70] Laboratoire de Physique Corpusculaire (LPC), Clermont Université, Université Blaise Pascal, CNRS-IN2P3, Clermont-Ferrand, France
[71] Laboratoire de Physique Subatomique et de Cosmologie, Université Grenoble-Alpes, CNRS-IN2P3, Grenoble, France
[72] Laboratori Nazionali di Frascati, INFN, Frascati, Italy
[73] Laboratori Nazionali di Legnaro, INFN, Legnaro, Italy
[74] Lawrence Berkeley National Laboratory, Berkeley, CA, United States
[75] Moscow Engineering Physics Institute, Moscow, Russia
[76] Nagasaki Institute of Applied Science, Nagasaki, Japan
[77] National Centre for Nuclear Studies, Warsaw, Poland
[78] National Institute for Physics and Nuclear Engineering, Bucharest, Romania
[79] National Institute of Science Education and Research, Bhubaneswar, India
[80] National Research Centre Kurchatov Institute, Moscow, Russia
[81] Niels Bohr Institute, University of Copenhagen, Copenhagen, Denmark
[82] Nikhef, Nationaal instituut voor subatomaire fysica, Amsterdam, Netherlands
[83] Nuclear Physics Group, STFC Daresbury Laboratory, Daresbury, United Kingdom
[84] Nuclear Physics Institute, Academy of Sciences of the Czech Republic, Řež u Prahy, Czech Republic
[85] Oak Ridge National Laboratory, Oak Ridge, TN, United States
[86] Petersburg Nuclear Physics Institute, Gatchina, Russia
[87] Physics Department, Creighton University, Omaha, NE, United States
[88] Physics Department, Panjab University, Chandigarh, India
[89] Physics Department, University of Athens, Athens, Greece
[90] Physics Department, University of Cape Town, Cape Town, South Africa
[91] Physics Department, University of Jammu, Jammu, India
[92] Physics Department, University of Rajasthan, Jaipur, India
[93] Physik Department, Technische Universität München, Munich, Germany
[94] Physikalisches Institut, Ruprecht-Karls-Universität Heidelberg, Heidelberg, Germany
[95] Purdue University, West Lafayette, IN, United States
[96] Pusan National University, Pusan, South Korea
[97] Research Division and ExtreMe Matter Institute EMMI, GSI Helmholtzzentrum für Schwerionenforschung, Darmstadt, Germany
[98] Rudjer Bošković Institute, Zagreb, Croatia
[99] Russian Federal Nuclear Center (VNIIEF), Sarov, Russia
[100] Saha Institute of Nuclear Physics, Kolkata, India
[101] School of Physics and Astronomy, University of Birmingham, Birmingham, United Kingdom
[102] Sección Física, Departamento de Ciencias, Pontificia Universidad Católica del Perú, Lima, Peru
[103] Sezione INFN, Bari, Italy
[104] Sezione INFN, Bologna, Italy
[105] Sezione INFN, Cagliari, Italy
[106] Sezione INFN, Catania, Italy
[107] Sezione INFN, Padova, Italy
[108] Sezione INFN, Rome, Italy
[109] Sezione INFN, Trieste, Italy
[110] Sezione INFN, Turin, Italy
[111] SSC IHEP of NRC Kurchatov institute, Protvino, Russia
[112] Stefan Meyer Institut für Subatomare Physik (SMI), Vienna, Austria
[113] SUBATECH, Ecole des Mines de Nantes, Université de Nantes, CNRS-IN2P3, Nantes, France
[114] Suranaree University of Technology, Nakhon Ratchasima, Thailand
[115] Technical University of Košice, Košice, Slovakia
[116] Technical University of Split FESB, Split, Croatia
[117] The Henryk Niewodniczanski Institute of Nuclear Physics, Polish Academy of Sciences, Cracow, Poland
[118] The University of Texas at Austin, Physics Department, Austin, TX, USA
[119] Universidad Autónoma de Sinaloa, Culiacán, Mexico
[120] Universidade de São Paulo (USP), São Paulo, Brazil
[121] Universidade Estadual de Campinas (UNICAMP), Campinas, Brazil
[122] University of Houston, Houston, TX, United States
[123] University of Jyväskylä, Jyväskylä, Finland
[124] University of Liverpool, Liverpool, United Kingdom
[125] University of Tennessee, Knoxville, TN, United States
[126] University of the Witwatersrand, Johannesburg, South Africa
[127] University of Tokyo, Tokyo, Japan
[128] University of Tsukuba, Tsukuba, Japan
[129] University of Zagreb, Zagreb, Croatia
[130] Université de Lyon, Université Lyon 1, CNRS/IN2P3, IPN-Lyon, Villeurbanne, France
[131] V. Fock Institute for Physics, St. Petersburg State University, St. Petersburg, Russia
[132] Variable Energy Cyclotron Centre, Kolkata, India
[133] Warsaw University of Technology, Warsaw, Poland
[134] Wayne State University, Detroit, MI, United States
[135] Wigner Research Centre for Physics, Hungarian Academy of Sciences, Budapest, Hungary
[136] Yale University, New Haven, CT, United States

[137] *Yonsei University, Seoul, South Korea*
[138] *Zentrum für Technologietransfer und Telekommunikation (ZTT), Fachhochschule Worms, Worms, Germany*

[i] Deceased.
[ii] Also at: Georgia State University, Atlanta, Georgia, United States.
[iii] Also at: Department of Applied Physics, Aligarh Muslim University, Aligarh, India.
[iv] Also at: M.V. Lomonosov Moscow State University, D.V. Skobeltsyn Institute of Nuclear Physics, Moscow, Russia.